Physical Aging in Poly(Methyl Methacrylate) / Poly(Styrene-co-Acrylonitrile) Blends. I. Stress Relaxation

JOVAN MIJOVIC,* STEVEN T. DEVINE,† and TAI HO,

Polytechnic University, 333 Jay Street, Brooklyn, New York 11201

Synopsis

An investigation was carried out on the effect of physical aging on viscoelastic properties of compatible polymer blends. Poly(methyl methacrylate) (PMMA) and poly(styrene-co-acrylonitrile) (SAN) were chosen for this study. Blends of six different ratios of PMMA and SAN were physically aged at different times and temperatures and then subjected to stress–relaxation tests at small strains. It was found that the shape of the stress–relaxation curve does not change with a change in blend composition, aging temperature, or aging time. A single "master curve" is presented, to which all data may be fit using 0.408 for the exponential parameter of the Williams–Watts equation. In creating the master curve, all data are shifted horizontally in time only. For a given set of experimental conditions, the relaxation time τ may be expressed in terms of blend composition, aging temperature, and aging time.

INTRODUCTION

It has been recognized for some time that, immediately upon cooling to below their glass transition temperature, polymers are characterized by departure from the equilibrium chain conformation. The ensuing drive toward equilibrium in the glassy state, which occurs with time, is referred to as "physical aging." On the molecular level, this approach toward equilibrium entails a continuation of molecular relaxations and a simultaneous decrease in free volume. Several theoretical approaches to modeling the process of physical aging have been reported in the literature.[1-7] The four most common experimental methods of monitoring physical aging include dilatometric,[1] calorimetric,[8] spectroscopic,[9] and viscoelastic[10] measurements.

Although the phenomenon of physical aging has been studied in glassy thermoplastics[11-16] and, more recently, thermosets,[17-22] limited information exists on aging of polymer blends, a major emerging new class of materials. The herein reported results focus on physical aging of a compatible polymer blend and are a part of our comprehensive research program on aging of polymer blends, supported by the National Science Foundation under the Materials Research Group (MRG) Grant. In this study, a series of blends of polymethyl methacrylate (PMMA) and poly(styrene-co-acrylonitrile) (SAN) were prepared and aged and their viscoelastic properties evaluated. The choice

---

*To whom correspondence should be addressed.
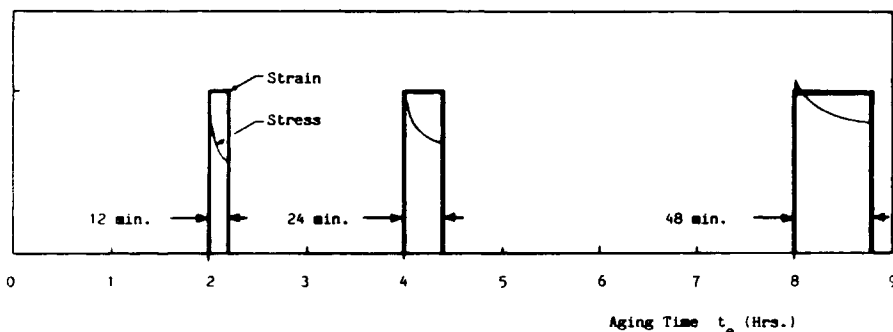†Currently with Pall Corporation, Glen Cove, NY.

Fig. 1. Schematic of stress–relaxation testing time and physical aging time.

of the PMMA/SAN system was based on three important points:

1. Availability of each component.
2. Compatibility of components in all blend ratios.
3. Glass transition and experimental conditions in an accessible temperature range.

The glass transition temperature (T_g) of each blend was determined using differential scanning calorimetry (DSC).

The main objectives of this study was to investigate the effect of physical aging on stress–relaxation characteristics of a series of PMMA/SAN blends. This was done at three different aging times, and three different temperatures, below T_g. The physical aging and stress–relaxation testing sequence chosen for this experiment was similar to that used by Struik,[10] and is schematically pictured in Figure 1. Each stress–relaxation period is short in comparison with the aging time, thus minimizing the effect of aging during the measurement.

EXPERIMENTAL

Materials

The samples of PMMA and SAN used in this study were obtained from commercial sources and their characteristics are shown in Table I. The SAN was Tyril 1000, natural, obtained from Dow Chemical Corp., and the PMMA was Plexiglas VS-100, obtained from Rohm-Haas.

Sample Preparation

Pellets of "as received" PMMA and SAN were mixed, processed in a twin screw extruder, and repelletized (courtesy of Werner-Pfleiderer Corp.). The resulting pellets were used to make test samples. Blend ratios produced by this method are listed in Table II.

Pellets of various compositions were dried in a vacuum oven overnight and then molded into sheets. The mold was comprised of three aluminum plates, with the top and bottom plates flat and free of flaws. The center plate, or

TABLE I
Description of Materials[a]

		M_n	M^*	M_w
SAN	Tyril 1000	72,000	—	150,000
PMMA	Plexiglas VS-100	67,000	75,000	—
where				
m_n = number average molecular weight				
M^* = intrinsic viscosity average molecular weight				
M_w = weight average molecular weight				

[a] The acrylonitrile content in SAN was 25.3%. The molecular weight of PMMA was measured by intrinsic viscosity.

TABLE II
Weight Composition of SAN/PMMA Blends Used in This Study

Sample No.	PMMA (wt%)	SAN (wt%)
1	100	0
2	80	20
3	60	40
4	40	60
5	20	80
6	0	100

"mask," was a rectangular border with the center cut out. This frame acted as a spacer, and a dam, to produce sheets of uniform length, width, and thickness. A measured volume of pellets was placed between the top and bottom plate and within the boundaries of the mask. The entire assembly was placed between the platens of a hydraulic press heated to approximately 200°C. Sufficient time was allowed for uniform melting eliminate voids before full pressure was applied. The assembly was then removed and immersed in water to quench from the melt. The resulting sheet was then removed from the center frame, labeled, and stored for future use.

Standard sample types used for tensile testing are described in ASTM D 638-82a. Type II was chosen for this study. Specimens were machined from sheet polymer by cutting into 3/4 in. wide strips. Each strip was then clamped in a jig of the desired final shape. Excess material was trimmed off using a router, resulting in a specimen suitable for testing. A minimum of two specimens were obtained from each sheet. They were stored in a polyethylene bag, with no special treatment, until pretest conditioning.

Experimental Techniques

Pre-test conditioning consisted of two distinct operations:

1. Above T_g annealing to relieve residual stress and contributions of previous physical aging.
2. Quenching.

Sample clip

Copper tube, 1" I.D.

Sample

Dry ice

Insulating foam cover
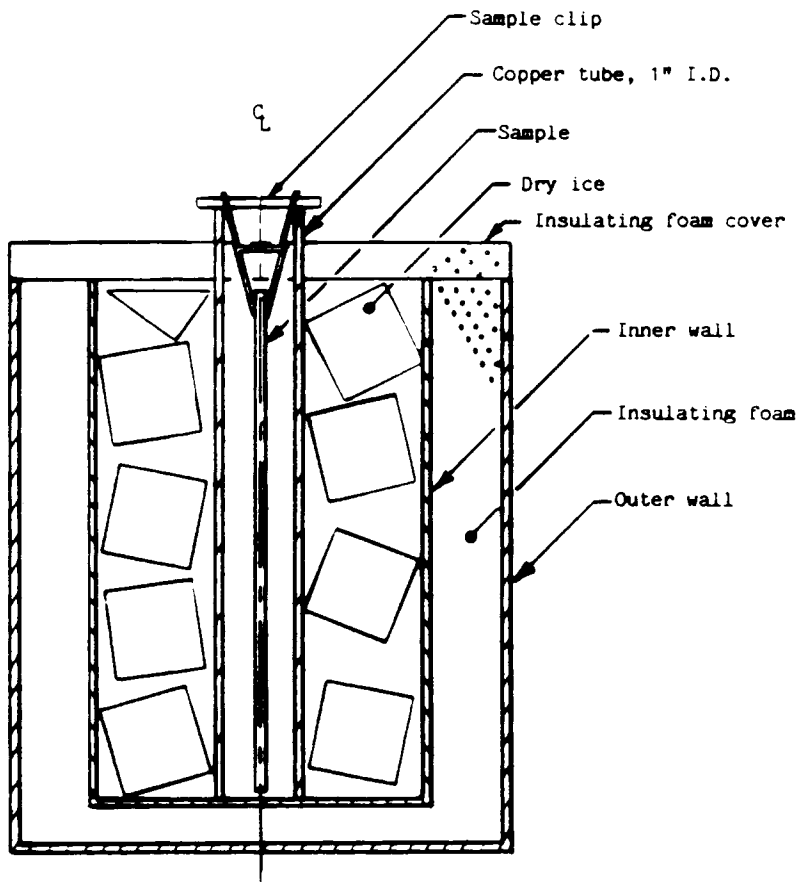
Inner wall

Insulating foam

Outer wall

Fig. 2. Sample quenching chamber.

The annealing step involved placing the specimen on a flat aluminum plate inside an oven preheated to 120°C. This condition was maintained for at least 30 min. Rapid quenching was achieved by hanging the sample vertically in a tube surrounded by dry ice. This technique resulted in uniform cooling of the sample with a minimum of the warping (out-of-plane deformation) or bending (in-plane deformation) usually associated with residual stress. In cases where the sample became warped or bent by more than 0.100 in., the annealing and quenching procedure was repeated until satisfactory results were achieved. A sketch of the sample quenching chamber is shown in Figure 2. After at least 2 min in the quenching apparatus, the sample width and thickness were measured in three places using a micrometer. The sample was then immediately fastened into the Instron grips within the environmental control chamber. A stop watch, indicating aging time, was started as soon as the door to the environmental control chamber was closed.

A precisely calibrated environmental control chamber was located in its operating position, and clamped firmly to the Instron loading frame. The grip distance was set to 5.300 in., and a previously calibrated mercury thermometer was placed approximately one inch in front of the upper grip. An expend-

TABLE III
Physical Aging and Stress–Relaxation Testing Temperatures for
Each Blend Composition at 20, 35, and 50°C below T_g

SAN (%)	T_g (°C)	$T_g - 20$ (°C)	$T_g - 35$ (°C)	$T_g - 50$ (°C)
0	94	74	59	44
20	97	77	62	47
40	100	80	65	50
60	103	83	68	53
80	104	84	69	54
100	106	86	71	56

able specimen of PMMA was placed between the grips. A minimum of 20 min was allowed for the temperature within the environmental control chamber to stabilize after each setpoint adjustment, whereupon the final datum point was recorded. Curves produced using progressively increasing and progressively decreasing setpoints were indistinguishable, indicating virtually no hysteresis.

The glass transition temperature (T_g) of each blend was determined in another study[23] using DSC at a heating rate of 10°C/min. Each blend composition exhibited a different T_g. In this study we observed the effects of physical aging at fixed intervals of temperature below the glass transition temperature for each blend. These increments were arbitrarily chosen to be 20, 35, and 50°C. Therefore, a total of 18 different aging temperatures were required. The glass transition temperature and the experimental target temperatures for each of the six blend compositions are listed in Table III. The environmental control chamber was preheated to the desired experimental temperature condition. The chamber was allowed to stabilize overnight and any final adjustments were made while the test specimen was being annealed. After quenching, the specimen was quickly transferred to the environmental chamber and centered between the grips. The upper grip was tightened before the lower grip to help ensure correct alignment. The temperature of the environmental chamber was controlled to ±0.2°C during data acquisition. A schematic representation of the general method of sequential aging and testing is shown in Figure 3. The symbols contained in Figure 3 are:

σ_0' = first approximation of σ_0 by manual extrapolation
t_0 = time at which strain is applied at a constant rate
t_s = time at which a constant strain is attained
t_1 = time at which the first acceptable datum point may be collected
t_{term} = time at which data are no longer collected

For the purpose of this experiment the following conditions were met:
1. $t_s = t_0 + 0.50$ min
At our experimental strain rate of 0.040 in./min, strain application for 0.50 min resulted in an elongation of 0.020 in.
2. $t_1 > 10(t_s)$
3. $t_{term} < t_e$(aging time)/10
For the entire series of experiments, the strain rate of 0.040 in./min was applied for a period of 30 (±1) s. The period of constant strain application
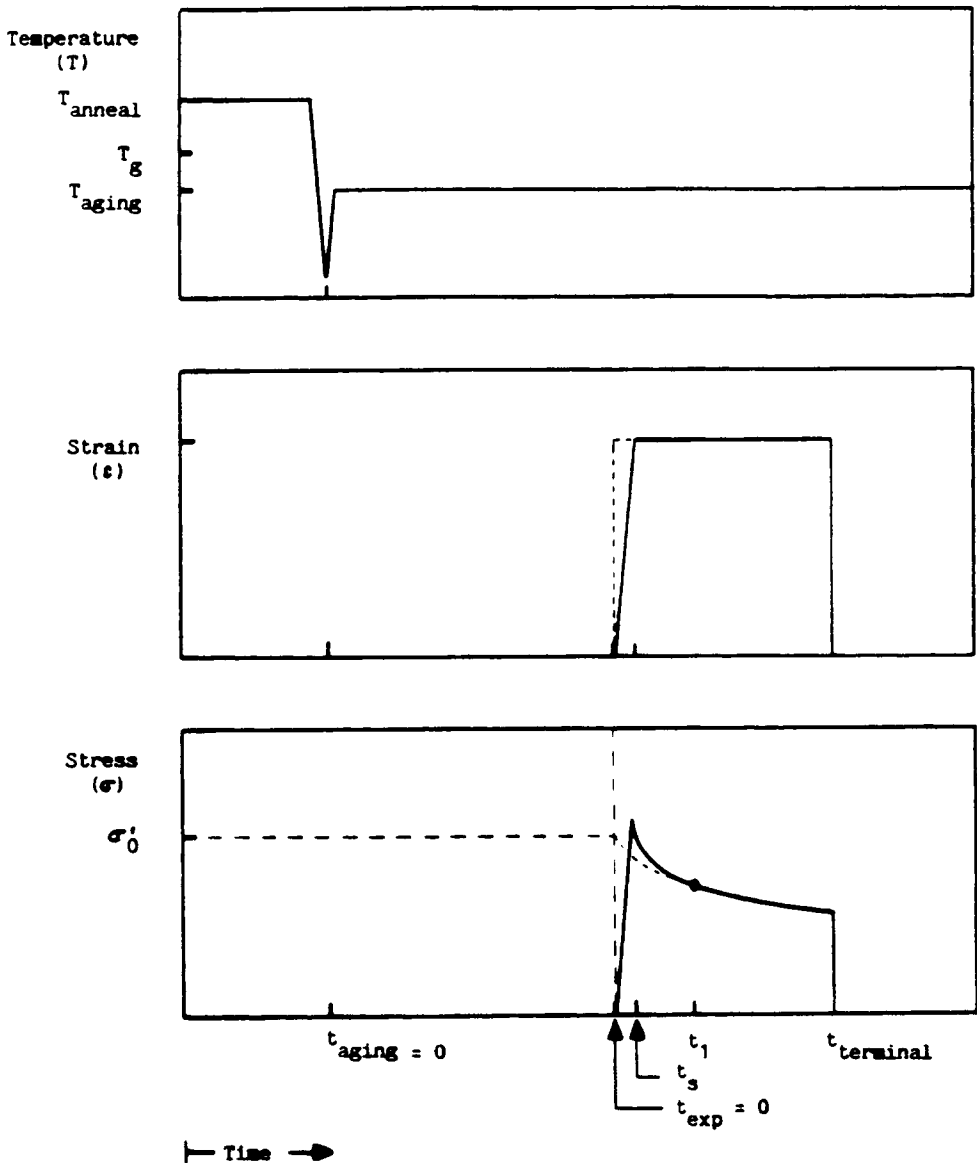
Fig. 3. Schematic representation of temperature, strain, and stress program for a single aging time test.

was timed with a stop watch and controlled manually. This was considered adequate since (1) the total strain applied was well within the linear viscoelastic region and (2) all data were normalized by dividing the force at a given experimental time by the force at experimental time zero. During the course of this experimentation, the Instron loading frame and control panel were modified to allow interfacing to an IBM personal computer for full information of the test.

RESULTS AND DISCUSSION

As an example of our results, a stress–relaxation trace for a 100% PMMA sample tested after 8 h of aging at $T_g - 20°C$ is shown in Figure 4. Experimental times at which data points were collected fell within the following guidelines:

1. Since it was not possible to instantaneously apply a finite strain to the sample, the strain was applied over a period of 0.5 min. The initial trial value of E_0' was determined by extrapolation to zero time.
2. Data recorded within the first 5 min after the initial application of strain were not used in calculations. Following the method used by Smith,[24] a delay of 1 order of magnitude greater than the time interval over which stress is applied is chosen to ensure that a true state of stress is being observed.
3. Data acquisition was terminated at a time equal to one tenth of the aging time at the start of the stress–relaxation experiment. We assumed that the contribution of physical aging while the stress–relaxation experiment proceeded was negligible.

The experimental time and the corresponding tensile force data were collected and stored on a computer diskette. For each blend we attempted to fit data recorded at three different aging times and three different temperatures below the glass transition temperature, using the well-known Williams–Watts relaxation function[25]:

$$\varphi_{(t)} = E_{(t)}/E_0 = e^{-(t/\tau)^\beta} \tag{1}$$

The Williams–Watts equation was originally used to describe nonsymmetrical dielectric relaxation behavior and has since been used to describe relaxation in a variety of glasses. Rearrangement of the Williams–Watts equation yields

$$-\ln \varphi_{(t)} = (t/\tau)^\beta \tag{2}$$

$$\ln(-\ln \varphi_{(t)}) = \beta(\ln t - \ln \tau) \tag{3}$$

A plot of $\ln(-\ln \varphi_{(t)})$ vs. $\ln t$ will yield a straight line of slope $= \beta$ and intercept $= -\beta \ln \tau$.

Initially, a value for E_0' was determined by extrapolation of the stress–relaxation trace to experimental time zero. This initial value of E_0', determined for each experiment, was used to calculate β and τ. The resulting values of β for all experiments were found to lie within a narrow range around 0.408. We then proceeded to calculate a value for E_0 based on this value for β by linear regression. Our magnitude of β lies between the 0.333 value proposed by Struik[10] and the 0.500 value proposed by Rekhson and Mazurin.[26] Struik's was determined by creep experiments on a wide range of amorphous polymers and other materials, whereas the Rekhson and Mazurin exponent resulted from stress–relaxation studies on inorganic glasses with metal inserts using a unique apparatus referred to as a "Relaxometer."

For each blend, plots of $E_{(t)}/E_0$ vs. t_{exp} were constructed for each aging time and temperature. These are shown in Figures 5–10. All of these plots
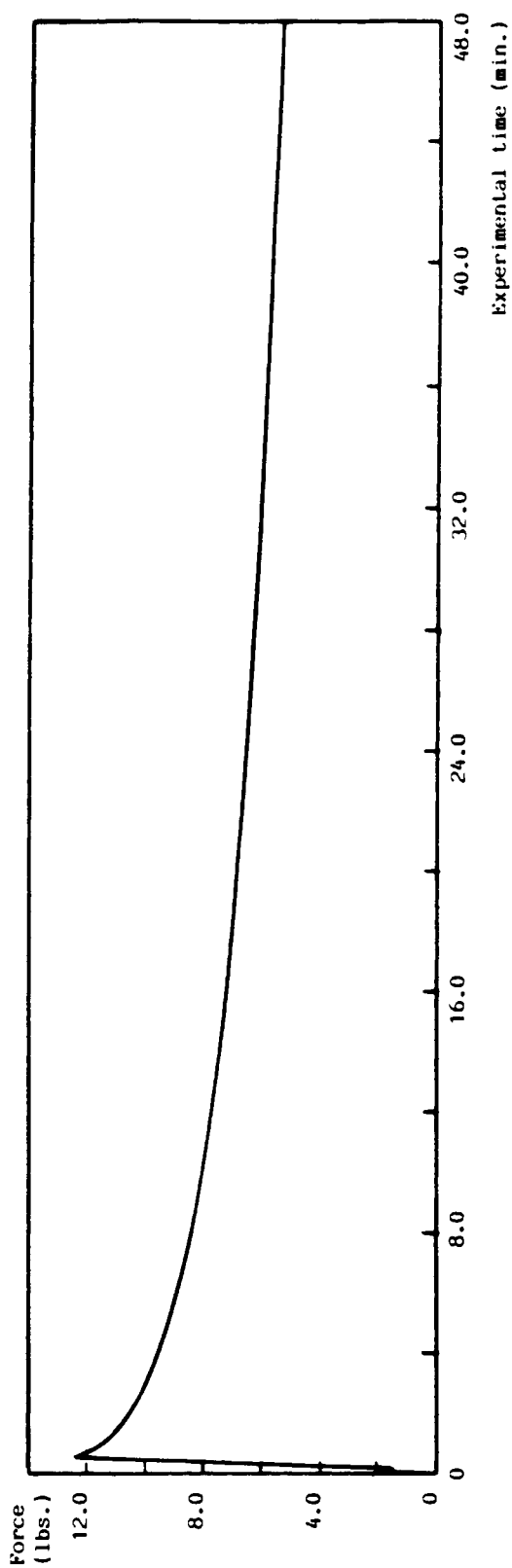
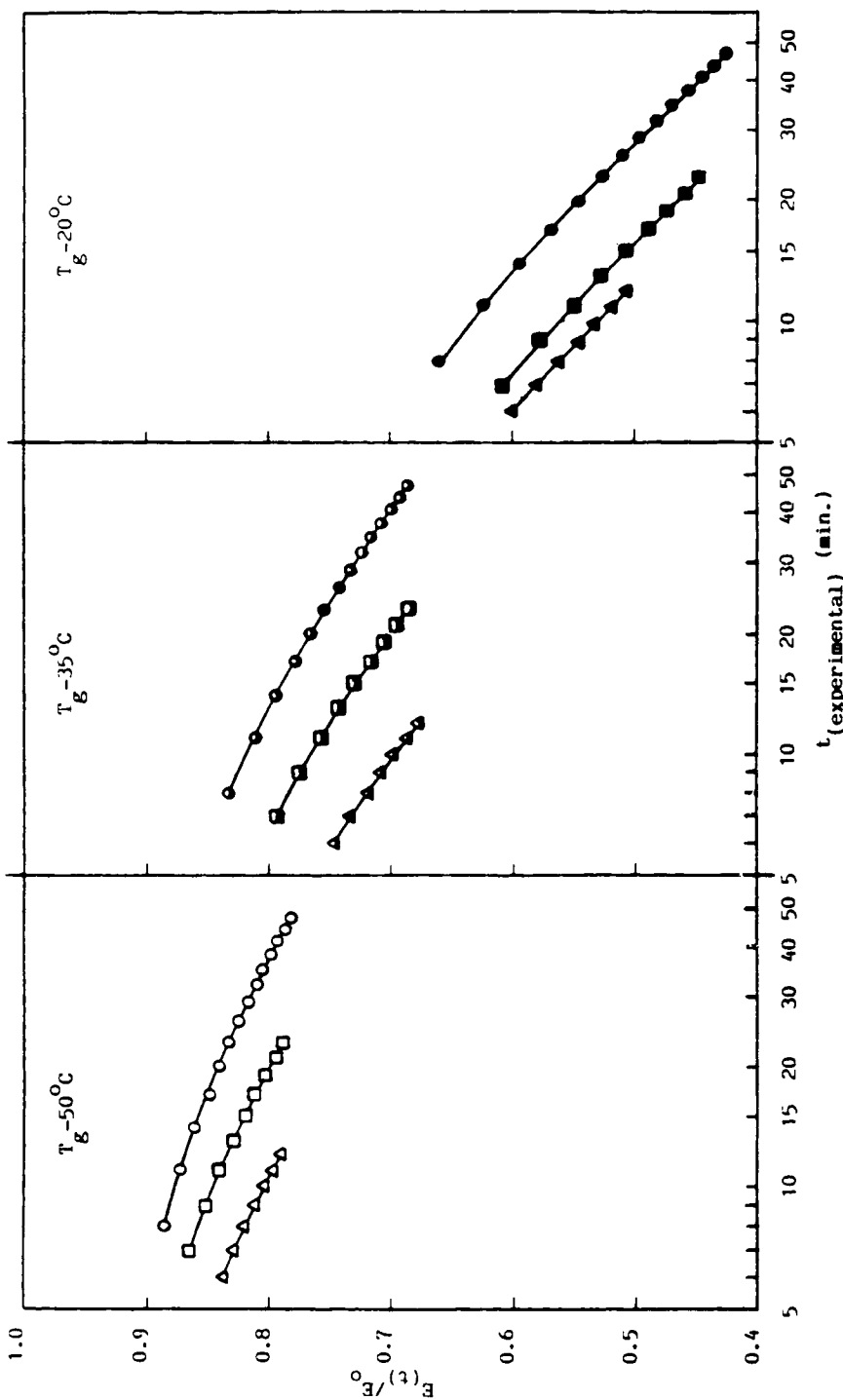Fig. 4.   Stress–relaxation trace for a 100% PMMA specimen tested after 8 hours of aging at $T_g - 20°C$.

Fig. 5. Normalized relaxation moduli for PMMA for different aging times (h): (○) 8; (□) 4; (△) 2; hollow point = $T_g - 20°C$; half-solid point = $T_g - 35°C$; solid point = $T_g - 50°C$.
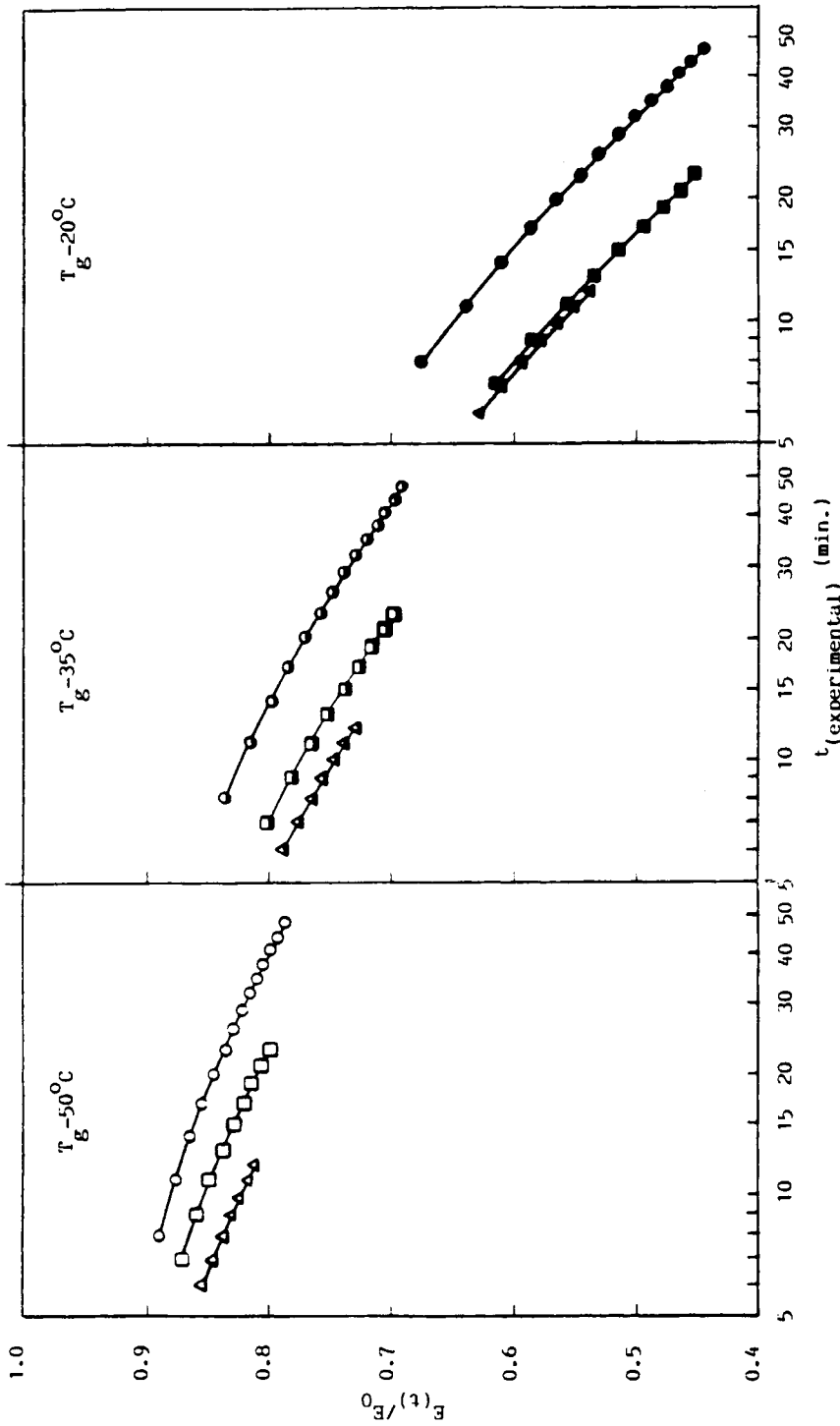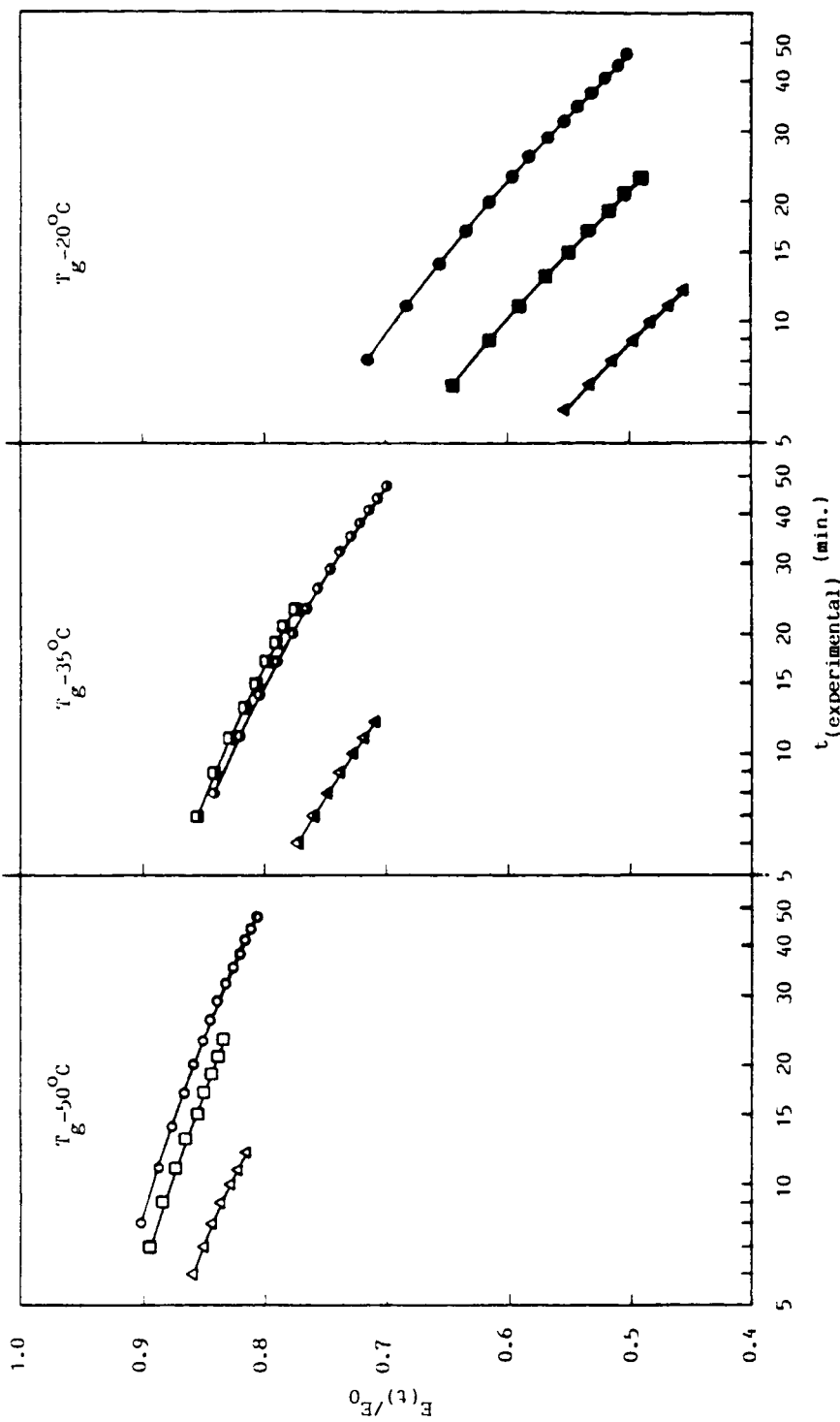
Fig. 6.   Normalized relaxation moduli for 80/20 PMMA/SAN blend. Key: same as Figure 5.

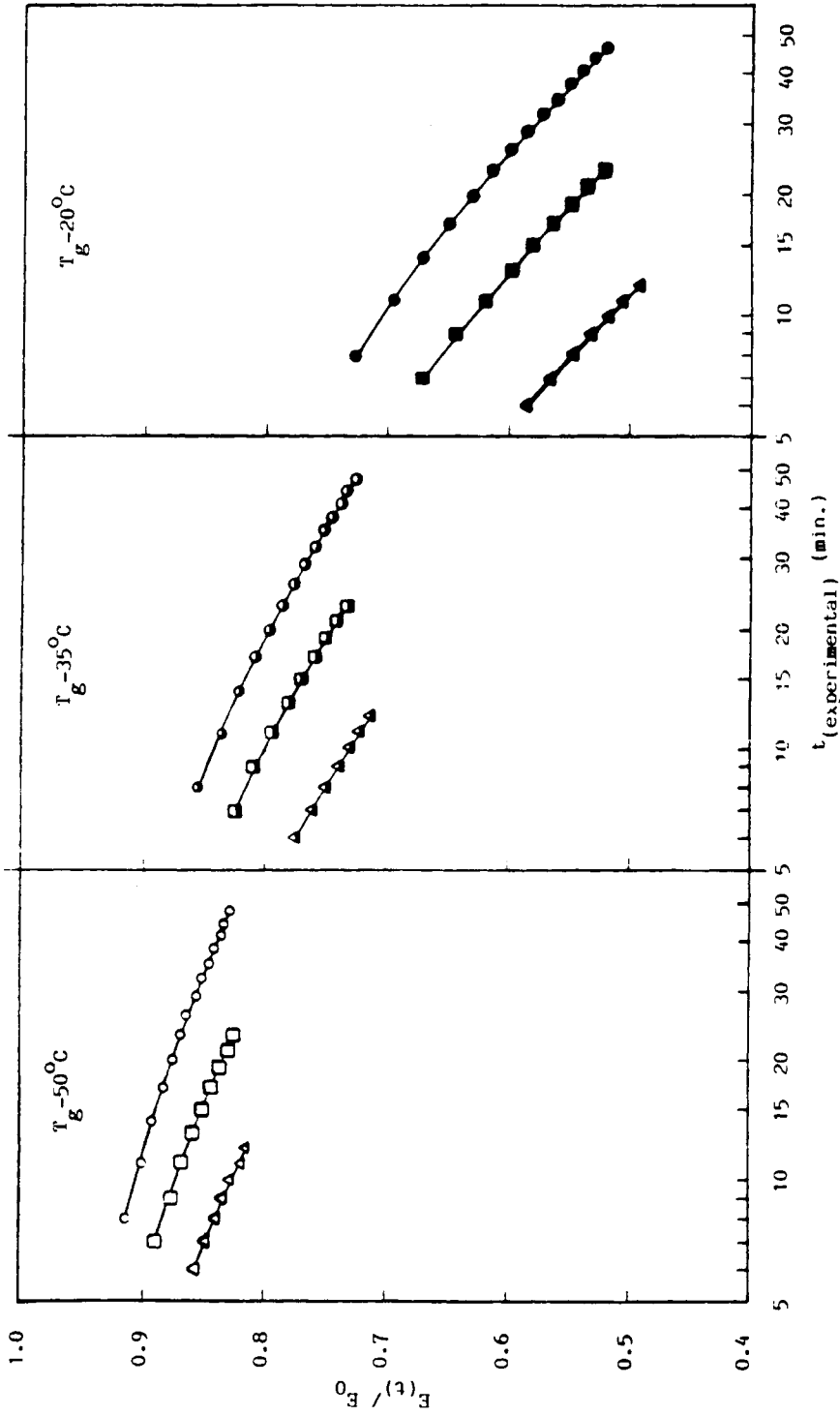Fig. 7.   Normalized relaxation moduli for 60/40 PMMA/SAN blend. Key: same as Figure 5.

Fig. 8.　Normalized relaxation moduli for 40/60 PMMA/SAN blend. Key: same as Figure 5.
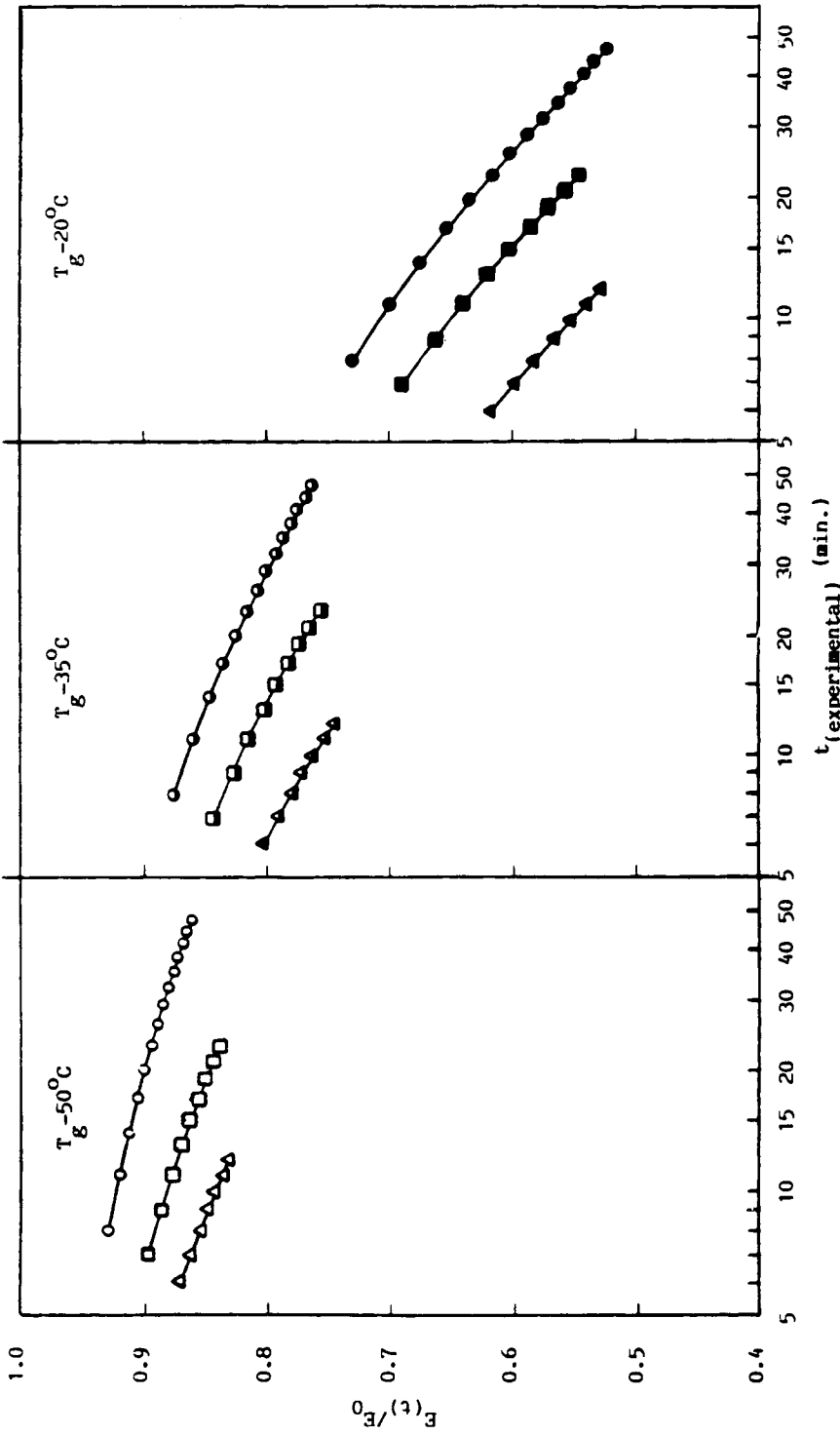
Fig. 9. Normalized relaxation moduli for 20/80 PMMA/SAN blend. Key: same as Figure 5.
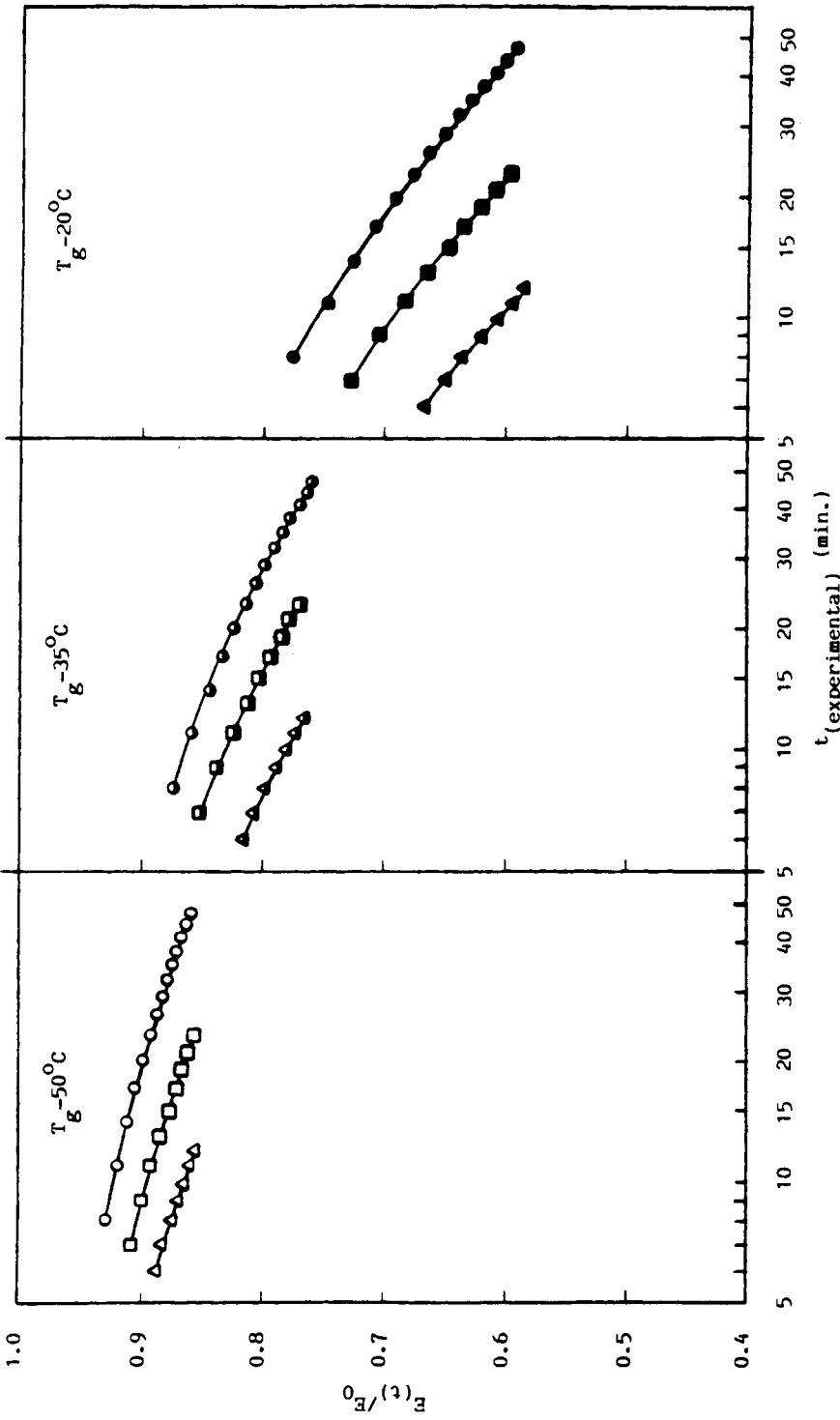
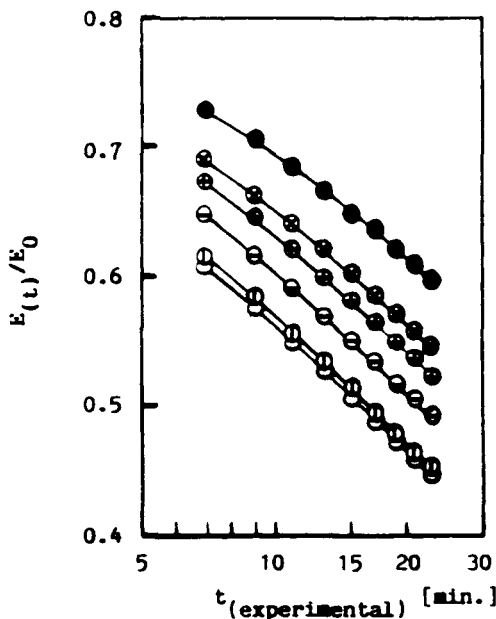Fig. 10. Normalized relaxation moduli for SAN. Key: same as Figure 5.

Fig. 11.   Normalized relaxation moduli obtained after 4 h of aging at $T_g - 20°C$: (○) 100% PMMA; (⊙) 80/20 PMMA/SAN; (⊖) 60/40 PMMA/SAN; (⊕) 40/60 PMMA/SAN; (⊗) 20/80 PMMA/SAN; (●) 100% SAN.

exhibit the same general features. Looking at Figure 5, for example, we notice that the relaxation modulus decreases with experimental time. At any given experimental time, the modulus increases with aging time. Naturally, for a given aging time, the modulus decreases with increasing temperature. By comparing plots of different blend compositions we see that the modulus of the sample, at a given aging time, temperature, and experimental time, generally increases as the weight percent of SAN increases. To illustrate this point, stress–relaxation curves for specimens of each blend ratio investigated that were subjected to 4 h aging time at a temperature of $T_g - 20°C$ were plotted on a single set of axes. This plot is shown in Figure 11.

The data plotted in Figures 5–10 may be shifted horizontally dividing the experimental time (t_{exp}) by the relaxation time (τ) on the time axis. Using the calculated values for τ and E_0, a single $E_{(t)}/E_0$ vs. t_{exp}/τ plot was made using data from each of the six blends, at the three temperature conditions and aging times. The plot obtained for 100% SAN is shown in Figure 12. The regions obtained at different temperatures are indicated above the curve and the regions obtained at different aging times for each temperature are indicated below the curve.

As shown in Figure 12, the upper (left) portion of the curve was derived from experiments conducted at low temperatures ($T_g - 50°C$) and the lower (right) portion of the curve resulted from experiments conducted at higher temperatures ($T_g - 20°C$). The superposition of all stress–relaxation data obtained for each blend at each aging time and temperature used in this study resulted in a single master curve shown in Figure 13. Relaxation times calculated for each of the 54 experimental conditions are shown in Table IV.
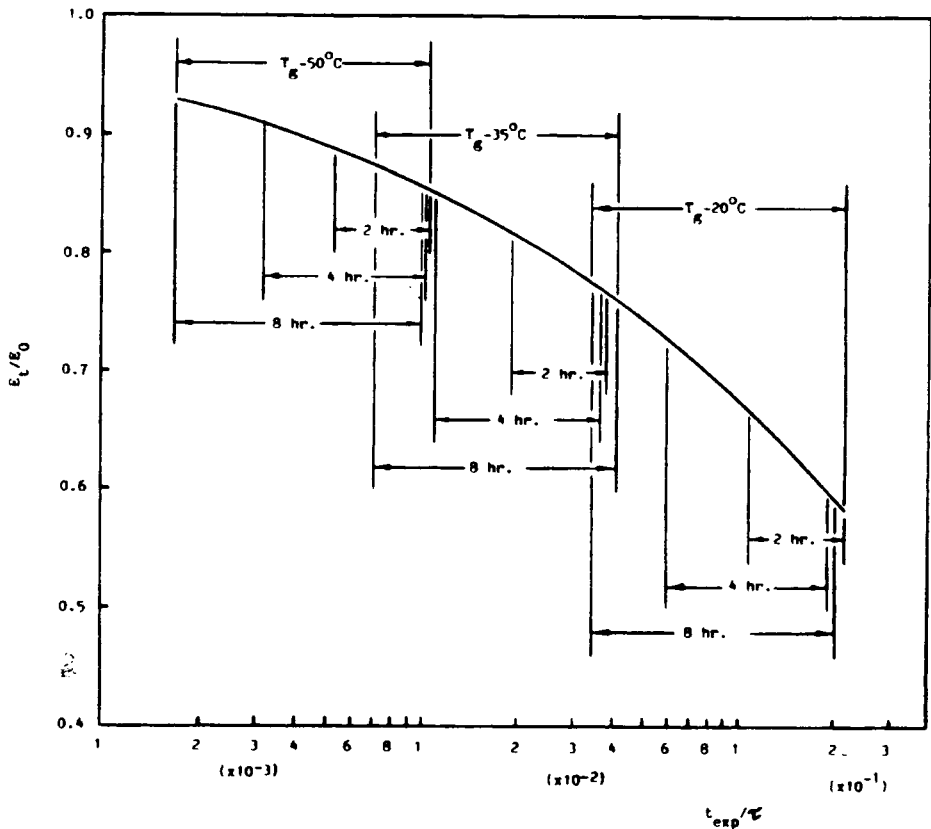
Fig. 12. Plot of $E_{(t)}/E_0$ vs. (t_{exp}/τ) for 100% SAN. The regions obtained at each aging temperature and time are indicated.

Our ability to superimpose all data plotted on the $E_{(t)}/E_0$ vs. t curves by the horizontal shift (obtained by plotting $E_{(t)}/E_0$ vs. t_{exp}/τ) indicates that a single expression relating to the blend composition, temperature, and aging time may exist.

An expression for τ that is suitable for the blends and the aging conditions studied has been suggested by Ho[23] and is shown as

$$\ln \tau = \mathbf{a} + b \ln\left(T_g - T_e\right) + c \ln t_e \tag{4}$$

where $\mathbf{a}$ is a function of the weight fraction of SAN in the blend. Function $\mathbf{a}$ is of the form

$$\mathbf{a} = a_1 + a_2 x + a_3 x^2 \tag{5}$$

Equations (4) and (5) contain the following symbols: a_1, a_2, and a_3 are constants, x = weight fraction of SAN, b = aging temperature parameter, c = aging time parameter, t_e = aging time, τ = relaxation time, T_g = glass transition temperature (°C), and T_e = aging temperature (°C). The derivation
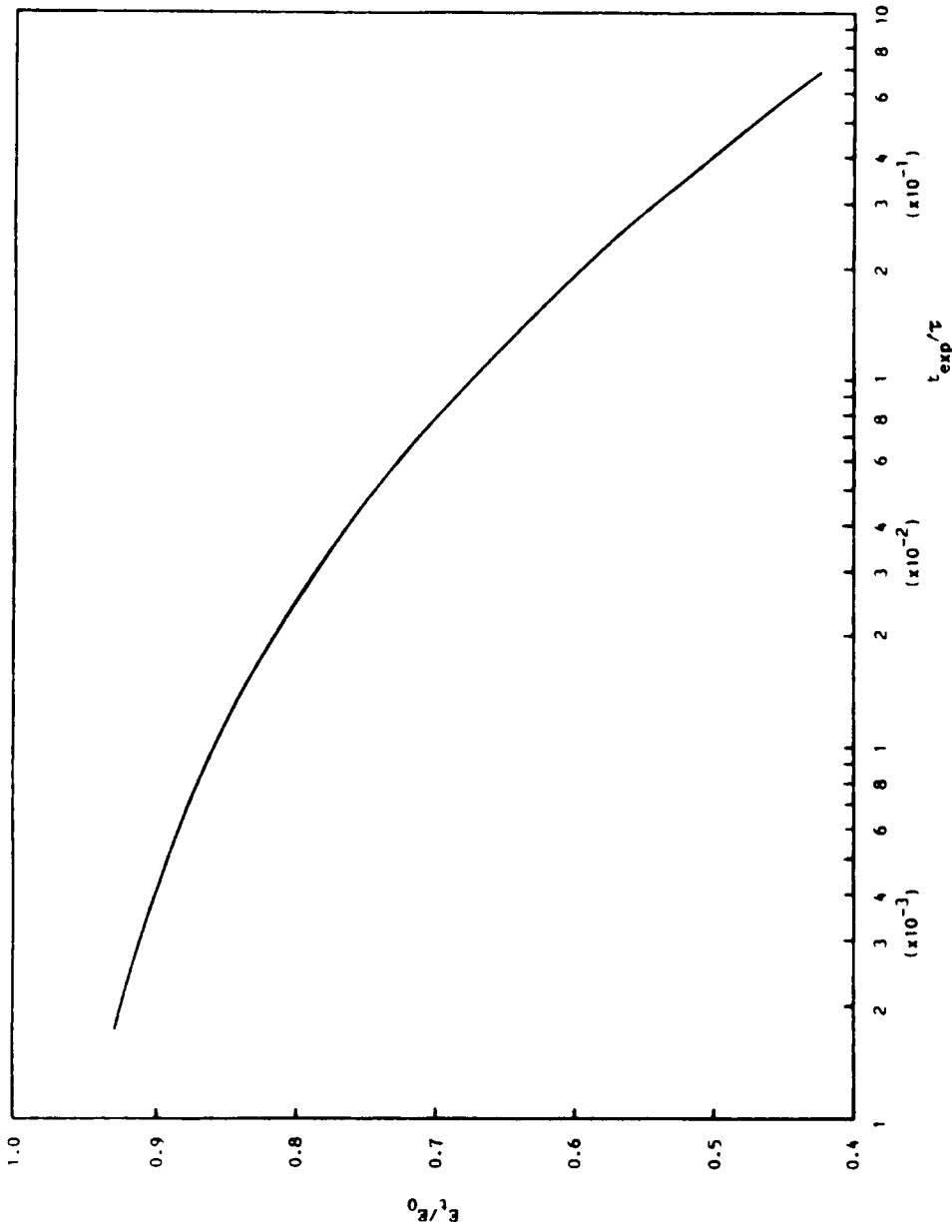
Fig. 13.   Master curve of all stress–relaxation data using $\beta = 0.408$.

TABLE IV
Relaxation Time τ at $\beta = 0.408$, as a Function of Blend
Composition and Aging Conditions

	% SAN					
	0	20	40	60	80	100
$T_g - 20$						
2	31	39	22	28	36	55
4	39	40	53	66	79	117
8	69	80	117	133	137	231
$T_g - 35$						
2	122	204	167	169	243	309
4	250	282	662	402	533	625
8	509	536	593	767	1136	1125
$T_g - 50$						
2	420	547	603	588	777	1131
4	797	906	1471	1318	1661	2196
8	1470	1561	2041	2848	5131	4718

of eqs. (4) and (5) and the determination of their parameters will be presented in a subsequent publication based on the work in progress.[23]

CONCLUSIONS

The Williams–Watts relaxation function was found to describe adequately the stress–relaxation response of PMMA/SAN blends undergoing physical aging below the glass transition temperature. The shapes of the individual stress–relaxation curves, expressed in terms of normalized relaxation modulus as a function of time ($E_{(t)}/E_0$ vs. t), did not change with composition, temperature, or aging time. This is reflected by the singular empirical value of 0.408 for the exponential (β) parameter in the Williams–Watts equation. Our value for β lies between that obtained from creep experiments by Struik (0.333) and that obtained from stress–relaxation experiments using a "Relaxometer" by Rekhson and Mazurin (0.500).

Superposition of stress–relaxation curves obtained under all experimental conditions was achieved by plotting the normalized relaxation modulus against the experimental time divided by the relaxation time (τ) [$E_{(t)}/E_0$ vs. (t/τ)]. The master curve shown in Figure 13 was obtained by shifting the individual stress–relaxation curves, for each blend, at each aging condition, horizontally along the time axis by the magnitude ($-\ln \tau$). The independence of β with respect to experimental conditions and the existence of a single master curve indicate that only the relaxation time is affected by the blend composition and the physical aging conditions. The relaxation times of each blend at each aging condition are unique, and may be related to sample composition, aging temperature, and aging time, using eq. (4) in the text.

References

1. A. J. Kovacs, *Fortschr. Hochpolym. Forsh.*, **3**, 394 (1963).
2. G. Adam and J. H. Gibbs, *J. Chem. Phys.*, **43**, 139 (1965).
3. O. S. Narayanaswamy, *J. Am. Ceram. Soc.*, **54**, 491 (1971).
4. C. T. Moynihan, et al., *Ann. NY Acad. Sci.*, **279**, 15 (1976).
5. T. S. Chow and W. M. Prest, Jr., *J. Appl. Phys.*, **53** (10), 6568 (1982).
6. I. M. Hodge, *Macromolecules*, **16**, 898 (1983).
7. S. Matsuoka, G. Williams, G. E. Johnson, E. W. Anderson, and T. Furukawa, *Macromolecules*, **18**, 2625 (1985).
8. S. E. B. Petrie, *J. Polym. Sci. A-2*, **10**, 1255 (1972).
9. B. L. Joss, R. S. Bretzlaff, and R. P. Wool, *J. Appl. Phys.*, **54**, 5515 (1983).
10. L. C. E. Struik, *Physical Aging in Amorphous Polymers and Other Materials*, Elsevier, Amsterdam, 1978.
11. K. Neki and P. H. Geil, *J. Macromol. Sci. Phys.*, **B8**, 295 (1973).
12. M. G. Wyzgoski, and G. S. Y. Yeh, *Int. J. Polym. Mater.*, **3**, 149 (1974).
13. R. Straff and D. R. Uhlmann, *J. Polym. Sci. Polym. Phys. Ed.*, **14**, 1087 (1976).
14. S. Matsuoka and H. E. Bair, *J. Appl. Phys.*, **48**, 4058 (1977).
15. A. J. Kovacs and J. M. Hutchinson, *J. Polym. Phys. Ed.*, **17**, 2031 (1979).
16. J. M. O'Reilly, *J. Appl. Phys.*, **50**, 6083 (1979).
17. Z. Ophir, J. A. Emerson, and G. L. Wilkes, *J. Appl. Phys.*, **49**, 5032 (1978).
18. J. Mijovic, *J. Appl. Polym. Sci.*, **27**, 1149 (1982).
19. J. Mijovic, *J. Appl. Polym. Sci.*, **27**, 2919 (1982).
20. E. S. W. Kong, S. M. Lee, and H. G. Nelson, *Polym. Compos.*, **3**, 29 (1982).
21. T. D. Chang and J. O. Brittain *Polym. Eng. Sci.*, **22**, 1121 (1982).
22. J. Mijovic and R. C. Liang, *Polym. Eng. Sci.*, **24**, 57 (1984).
23. T. Ho, Ph.D. Thesis, Polytechnic University, in progress.
24. T. L. Smith, *J. Polym. Sci.*, **17**, 2181 (1979).
25. G. Williams and D. C. Watts, *Trans. Farad. Soc.*, **66**, 80 (1970).
26. S. M. Rekhson and O. V. Mazurin, *Glass Technol.*, **13**, 1 (1977).